Generalization of the Lattice–Fluid Model for Specific Interactions

Isaac C. Sanchez*

Aluminum Company of America, Alcoa Center, Pennsylvania 15609

Anna C. Balazs

Materials Science & Engineering Department, University of Pittsburgh, Pittsburgh, Pennsylvania 15261. *Received September 12, 1988; Revised Manuscript Received October 25, 1988*

ABSTRACT: A strong or specific interaction between dissimilar components in a mixture has both an energetic and entropic component. The entropy contribution was ignored in the original lattice–fluid model but is included here in a systematic way. A critical comparison of the new theory is made with recent small-angle neutron-scattering data on the polymer blend system poly(vinyl methyl ether)/polystyrene. A quantitative description of the spinodal phase diagram, as well as a semiquantitative description of the composition and temperature dependence of the χ interaction parameter, is possible with the new theory. The inclusion of specific interactions and the associated entropy effects appear to have significantly improved the lattice–fluid model.

Introduction

Thermally induced phase separations in binary mixtures or lower critical solution temperature (LCST) phenomena have fascinated scientists for many years. LCSTs have been observed in strongly interacting polar mixtures as well as in weakly interacting nonpolar mixtures. Aqueous solutions are an example of the former, and nonpolar polymer solutions are excellent examples of the latter.

In recent years a clearer understanding of LCST behavior has emerged. The origins are 2-fold: strong or *specific interactions* between components and the mixture's *finite compressibility*. In either case a thermodynamic analysis indicates that the phase separation (transition) is entropically driven.[1-3] In nonpolar polymer solutions, compressibility effects are dominant, and both the Flory–Orwoll–Vrij–Eichinger (FOVE) equation of state model[4-7] and the lattice–fluid (LF) model[3,8-10] of Sanchez and Lacombe adequately describe LCST behavior in polymer solutions. In their original formulations, neither model took into account specific interactions and the associated entropy effects. Strong or specific interactions should induce some local ordering or degree of nonrandomness in a mixture.[11] Therefore, it is not surprising that in proceeding from nonpolar to slightly polar to strongly polar solutions that, in some applications, a gradual breakdown of the FOVE and LF models occurs.

In this paper the LF model is generalized to account for strongly interacting components. The basic idea is that for two components, say monomers on two different polymer chains, to interact strongly, they must be in the proper orientation with respect to one another; i.e., there is a specific spatial or geometric constraint on the interaction (hence, the terminology "specific interaction"). Other mutual orientations of the interacting pair are energetically less favorable, but many more of them may exist (rotational degrees of freedom). Thus, an entropic price must be paid to form the specific interaction.

Using quasi-chemical approaches to treat the nonrandom character of a solution, Panayiotou and Vera[12] and Renuncio and Prausnitz[13] have developed improved modifications of the FOVE model. Heretofore, a similar "upgrade" of the LF model has not been forthcoming, although recently Panayiotou[14] has generalized the LF model in the same spirit as the original FOVE model was formulated. One of the two new ad hoc parameters introduced is an entropy parameter (q_{12}) that, in principle, takes into account entropy effects that might occur with strongly interacting components. Here we adopt a more systematic approach for including these entropy effects.

* To whom correspondence should be addressed at Chemical Engineering Department and Center for Polymer Research, University of Texas, Austin, TX 78712.

Model Description

The philosophy that we have adopted is to generalize the LF model for specific interactions while trying to preserve its simplicity. Guggenheim's quasi-chemical approximation[15] does not satisfy our criterion for simplicity. Instead we have adopted a simpler approach that is quite similar to that of ten Brinke and Karasz, who have developed an incompressible model of binary mixtures with specific interactions.[16] The compressible version of the ten Brinke–Karasz model is essentially our generalized LF model.

To keep the arguments concrete, a lattice of coordination number z will be used to develop the model. At zero pressure the LF free energy f per mer of a binary mixture of N_1 molecules of size r_1 and N_2 molecules of size r_2 (a r-mer occupies r sites) is[8-10]

$$f = -\tilde{\rho}\epsilon^* - T(s_{comb} + s_{vac}) \tag{1}$$

where s_{comb} is the usual combinatorial entropy of mixing

$$-s_{comb}(\phi)/k = \frac{\phi_1}{r_1} \ln \phi_1 + \frac{\phi_2}{r_2} \ln \phi_2 \tag{2}$$

s_{vac} is the entropy of mixing lattice vacancies with the molecules

$$-s_{vac}(\tilde{\rho})/k = (1 - \tilde{\rho}) \ln (1 - \tilde{\rho})/\tilde{\rho} + \ln \tilde{\rho}/r \tag{3}$$

and ϵ^* is the mixing interaction energy

$$\epsilon^*(\phi) = (z/2)(\phi_1^2\epsilon_{11} + 2\phi_1\phi_2\epsilon_{12} + \phi_2^2\epsilon_{22}) \equiv \phi_1^2\epsilon^*_{11} + 2\phi_1\phi_2\epsilon^*_{12} + \phi_2^2\epsilon^*_{22} \tag{4}$$

$\tilde{\rho}$ is the reduced density of the mixture and equals the fraction of occupied sites, and $1 - \tilde{\rho}$ is the vacancy site fraction; ϕ_i is the volume fraction of the ith component at zero temperature ($\tilde{\rho} = 1$); ϵ_{ij} is the mer–mer interaction energy between mers i and j and is related to ϵ^*_{ij} by

$$\epsilon^*_{ij} \equiv z\epsilon_{ij}/2 \tag{5}$$

$$\frac{1}{r} = \frac{\phi_1}{r_1} + \frac{\phi_2}{r_2} \tag{6}$$

0024-9297/89/2222-2325$01.50/0

We now consider the case where the 1–2 interaction can be weak (nonspecific) with energy ϵ_{12} or strong (specific) with energy $\epsilon_{12} + \delta\epsilon$. If θ of the N_{12} interactions are strong and $1 - \theta$ are weak, then the total potential energy (E_{12})

$$E_{12} = -N_{12}[(1 - \theta)\epsilon_{12} + \theta(\epsilon_{12} + \delta\epsilon)] = -N_{12}(\epsilon_{12} + \theta\delta\epsilon) \quad (7)$$

If a specific 1–2 interaction can occur in only one unique way, let q be the number of ways that the nonspecific 1–2 interaction occurs. If the specific interaction can occur in more than one way, then q equals the ratio of the statistical degeneracies of the two states. Strictly specking, q should be related to the lattice coordination number z, but we adopt a more liberal interpretation of q and will treat it as a parameter independent of z. As will be seen later, its exact value is not important. The number of distinguishable arrangements of the N_{12} pairs on the lattice is $(1 + q)^{N_{12}}$. In the absence of energetic preferences the probability $P(\theta)$ that θ of these interactions are specific and $1 - \theta$ are nonspecific is given by the combinatorial expression

$$P(\theta) = \frac{N_{12}!}{(\theta N_{12})![(1 - \theta)N_{12}]!} \frac{q^{(1-\theta)N_{12}}}{(1 + q)^{N_{12}}} \quad (8)$$

Note that $\sum P(\theta) = 1$. The partition function Z_{12} associated with these 1–2 interactions is

$$Z_{12} = \sum_{\theta} P(\theta) \exp[+N_{12}\beta(\epsilon_{12} + \theta\delta\epsilon)] \quad (9)$$

where $\beta = 1/kT$. In a mean-field approximation with $\tilde{p}$ of the sites occupied, N_{12} is given by

$$N_{12} = z\tilde{p}(r_1N_1 + r_2N_2)\phi_1\phi_2 \quad (10)$$

Thus, the free energy (F_{12}) associated these 1–2 interactions is given by

$$F_{12} = -kT \ln Z_{12} = -N_{12}f_{12} \quad (11)$$

Approximating Z_{12} by the generic term in the sum defines f_{12} as

$$f_{12} = \epsilon_{12} + \theta\delta\epsilon - kT[\theta \ln \theta + (1 - \theta) \ln [(1 - \theta)/q] + \ln (1 + q)] \quad (12a)$$

The entropy associated with the formation of specific interactions equals k times the function of θ enclosed in brackets in eq 12a. Minimizing F_{12} with respect to θ yields

$$\theta = [1 + q \exp(-\beta\delta\epsilon)]^{-1} \quad (13)$$

From eq 13, f_{12} can be rewritten as a function of temperature:

$$f_{12} = \epsilon_{12} + \delta\epsilon - kT \ln \left[\frac{1 + q}{1 + q \exp(-\beta\delta\epsilon)}\right] \quad (12b)$$

Thus, the free energy associated with 1–2 interactions becomes

$$F_{12} = -z\tilde{p}(r_1N_1 + r_2N_2)\phi_1\phi_2f_{12} \quad (14)$$

and the generalized LF free energy (per mer) becomes

$$f = -\tilde{p}(\phi_1^2\epsilon^*_{11} + 2\phi_1\phi_2f^*_{12} + \phi_2^2\epsilon^*_{22}) - T(s_{comb} + s_{vac}) \quad (15)$$

where f^*_{12} is given by (cf. eq 5)

$$f^*_{12} \equiv zf_{12}/2 \quad (16)$$

Equation 15 is our main result. Comparing eq 15 with eq 1, we see that the purely energetic parameter ϵ^*_{12} has been replaced by the free energy parameter f^*_{12}. If $\tilde{p}$ is set to unity in eq 15 so that $s_{vac} = 0$ (this incompressible limit is approached at low temperatures), the ten Brinke–Karasz free energy[16] is recovered. If $\delta\epsilon = 0$, $f^*_{12} = \epsilon^*_{12}$ and eq 15 reduces to eq 1, the original LF free energy. In the trivial case of $q = 0$ (only the specific interaction is allowed), the free energy reduces again to the LF free energy.

The equation $\partial f/\partial\tilde{p})_{\phi} = 0$ determines the equilibrium value of $\tilde{p}$ and yields the familiar form

$$\tilde{p}^2\beta\epsilon^*_T + \ln (1 - \tilde{p}) + (1 - 1/r)\tilde{p} = 0 \quad (17a)$$

where ϵ^*_T is a function of composition and temperature:

$$\epsilon^*_T(\phi,T) = \phi_1^2\epsilon^*_{11} + 2\phi_1\phi_2f^*_{12}(T) + \phi_2^2\epsilon^*_{22} \quad (18)$$

Note that $\epsilon^*_T = \epsilon^*$ when $\delta\epsilon = 0$ (see eq 4 and 12b). Equation 17a can be rewritten more conveniently for numerical solution as

$$\tilde{p} = 1 - \exp[-\tilde{p}^2\beta\epsilon^*_T - (1 - 1/r)\tilde{p}] \quad (17b)$$

Phase Stability and Spinodal Diagrams

Knowledge of the free energy, eq 15, allows the construction of phase diagrams. For a binary mixture a homogeneous phase is thermodynamically stable or metastable if

$$d^2f/d\phi^2 > 0 \quad (19)$$

where $\phi = \phi_1$ or ϕ_2. The above inequality defines the spinodal region of the phase diagram. With ordinary differential calculus methods, it can be shown that[2,3]

$$\frac{d^2f}{d\phi^2} = f_{\phi\phi} + f_{\phi\tilde{p}}\frac{d\tilde{p}}{d\phi} = f_{\phi\phi} - f_{\phi\tilde{p}}^2f_{\tilde{p}\tilde{p}}^{-1} = \begin{vmatrix} f_{\phi\phi} & f_{\phi\tilde{p}} \\ f_{\phi\tilde{p}} & f_{\tilde{p}\tilde{p}} \end{vmatrix} f_{\tilde{p}\tilde{p}}^{-1} \quad (20)$$

where $f_{\phi\phi} = \partial^2f/\partial\phi^2$, $f_{\phi\tilde{p}} = \partial^2f/\partial\phi\partial\tilde{p}$, etc. These partial derivatives are taken by holding the other variable constant, and all are easily evaluated (see below). Since $\partial f/\partial\tilde{p} \equiv f_{\tilde{p}} = 0$ defines the free energy minimum and the equilibrium value of $\tilde{p}$ at zero pressure (eq 17), $f_{\tilde{p}\tilde{p}}$ must be positive (see eq 22 and 28). Thus, the condition for phase stability requires that the above determinant be positive. The conditions where the determinant is zero define the spinodal line.

The idea that the mixture's finite compressibility has an influence on phase behavior is demonstrated as follows: Using the thermodynamic identity $P = -(\partial F/\partial V)_T$, where F is the Helmholtz free energy, we find that

$$\rho^2f_{\tilde{p}} \sim P \quad (21)$$

where P is the system pressure, V is the volume, and ρ is density. Taking another density derivative on eq 21, it is easy to show that at low pressures (atmospheric pressure is low pressure)

$$f_{\tilde{p}\tilde{p}}^{-1} \sim \kappa\rho^3 > 0 \quad (22)$$

where $\kappa \equiv -(\partial \ln V/\partial P)_T$ is the isothermal compressibility of the mixture. Thus, from eq 19, 20, and 22, we see that the mixture's finite compressibility destabilizes the mixture and promotes phase separation. Since compressibility increases with temperature, this destabilization becomes more important with increasing temperature.

In our generalization of the LF model for specific interactions, we have introduced three new parameters: the coordination number (z) and the energy ($\delta\epsilon$) and entropy (q) parameters associated with the specific interactions. The coordination number also appears in the original LF model, but it is only a scale factor that is absorbed in the energy parameters as shown in eq 4. Here it scales not only the energies but also an entropy term as shown in eq 12a and 16. Although it must now be specified explicitly, it can be assigned any reasonable value ($z = 12$ in our cal-

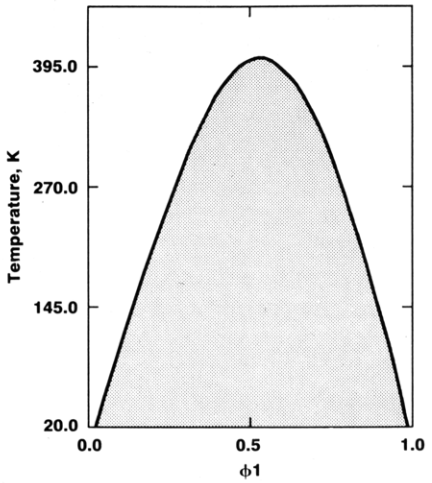

Figure 1. Typical UCST type phase diagram. The pure component parameters are $r_1 = 250$, $T^*_1 = 540$ K, and $r_2 = 190$, $T^*_2 = 600$ K. The interaction parameters are $\epsilon^*_{12}/k = 568.5$ K and $\delta\epsilon^* = 0$.

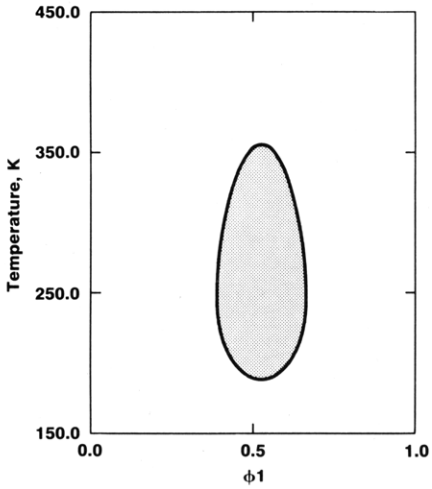

Figure 2. Closed immisicibility loop phase diagram. Pure component parameters are the same as in Figure 1. Interaction parameters are $\epsilon^*_{12}/k = 552$ K, $\delta\epsilon^* = 176.4$ K, and $q = 10$.

culations) and eliminated as an adjustable parameter. The energy parameter $\delta\epsilon$ is really not an independent parameter; its value depends on the value of the nonspecific interaction energy ϵ_{12} that is selected (this is the only adjustable parameter in the original LF model) and the value of q. Its dependence on ϵ_{12} is especially apparent at low temperatures. As absolute zero temperature is approached, both $\tilde{\rho}$ and θ approach unity, and all contributions to the free energy from entropy terms vanish. The thermodynamics of the system are completely controlled by energetics. The sign of the heat of mixing is determined by the sign of

$$\Delta\epsilon^* \equiv (z/2)[\epsilon_{11} + \epsilon_{22} - 2(\epsilon_{12} + \delta\epsilon)] \equiv \epsilon^*_{11} + \epsilon^*_{22} - 2(\epsilon^*_{12} + \delta\epsilon^*) \quad (23)$$

If $\Delta\epsilon^*$ is positive, then phase separation will always occur at low temperatures; if $\Delta\epsilon^*$ is negative or zero, then complete miscibility will be achieved at low enough temperatures even though at higher temperatures immiscibility may result (of course, in real systems freezing of the mixture sometimes intervenes before phase separation is observed). This kind of qualitative behavior is illustrated in Figures 1 and 2. In Figure 1 $\Delta\epsilon^*/k = 3.0$ K, and upper critical solution temperature (UCST) type behavior is observed. In Figure 2 the pure-component parameters are the same as in Figure 1, but now $\Delta\epsilon^*/k = -316.8$ K with $\delta\epsilon^*/k = 176.4$ K and $q = 10$. Notice that not only is LCST behavior observed but a closed immiscibility loop is obtained.

Table I
Equation of State Parameters and Molecular Weights[a]

	T^*, K	P^*, atm	ρ^*, g/cm^3
PVME	657	3580	1.10
PS	735	3530	1.19
	mol wt		r (size parameter)[b]
	Data Set 1		
PVME	389 000		23 400
PS	230 000		11 300
	Data Set 2		
PVME	1 100 000		66 200
PS	593 000		29 100

[a] PVME parameters calculated at 400 K by using $T\alpha = 0.2962$, $\gamma = 0.17$ cal/cm^3 K, and $\rho = 0.976$ g/cm^3 from ref 18. PS parameters taken from ref 9; correction of 112/104 applied to ρ^* to account for deuteration of PS. [b] Calculated according to eq 25.

Recently, Han et al.[17] using small-angle neutron scattering have carried out some very careful measurements of the spinodal line on well-characterized samples of the polymer blend system poly(vinyl methyl ether)/(deuterated)polystyrene (PVME/PS). This well-known system exhibits a LCST. To comapre these spinodal data with the present model, it is necessary to have the equation of state parameters for each component. For polystyrene these parameters are already tabulated.[9,10] Recently equation of state data were published for PVME,[18] which were used to compute the requisite PVME parameters. Both the PS and PVME parameters, the characteristic temperatures (T^*), pressures (P^*), and mass densities (ρ^*), used in our calculations are given in Table I. The interaction energies of each component (ϵ^*_{ii}) are related to the characteristic temperatures (T^*_i) by

$$\epsilon^*_{ii} \equiv kT^*_i \quad (24)$$

The size parameters r_i are calculated from

$$r = M(P^*/kT^*\rho^*) \quad (25)$$

where M is the molecular weight.

In Figure 3a the experimental spinodal data of Han et al.[17] are shown along with the calculated spinodal line for the unmodified LF model (no specific interactions, $\delta\epsilon = 0$). The weight average molecular weights are 2.3×10^5 for the deuterated PS and 3.89×10^5 for PVME (data set 1). There is only one parameter (ϵ^*_{12}) that is adjustable in this calculation. Notice that it was chosen so that $\Delta\epsilon^*$ was slightly negative.

There are two salient points: The first is that the calculated critical composition (ϕ_c) is very close to that observed experimentally. The adjustable parameter ϵ^*_{12} allows for the matching of the experimental LCST with the calculated one, but its value does not affect the critical composition. The critical composition is also relatively insensitive to the values of r_1 and r_2. For example, doubling the value of r_{PS} does not affect ϕ_c. Doubling the value of r_{PVME} slightly shifts ϕ_c to a richer PVME. In the classical theory of polymer solutions, which yields only an UCST, and in the ten Brinke–Karasz model, which yields both UCST and LCSTs, the ϕ_c is always rich in the component with the smaller size parameter r. Here the PS is lower in molecular weight and has the smaller value of r by a factor of 2; nevertheless, ϕ_c is richer in PVME. The LF model qualitatively predicts that ϕ_c for a LCST is rich in the component with the smaller ϵ^*_{ii}, which in our case is PVME. A detailed discussion of this effect is given in the next section.

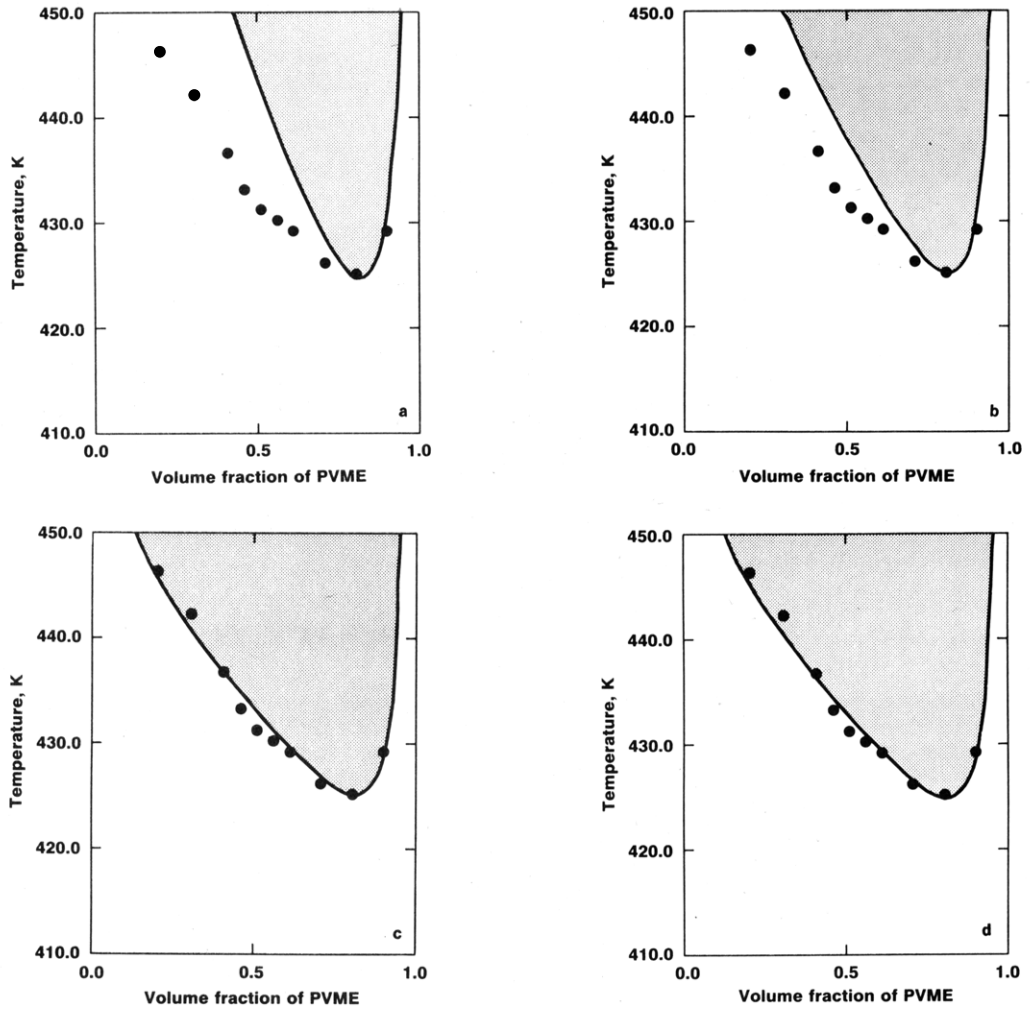

Figure 3. Comparison of experimental spinodal data[17] (solid circles, data set 1) and calculated spinodals for the PVME/PS system. Pure component parameters used in the calculations were all identical and are listed in Table I. Interaction parameters: (a) ϵ^*_{12}/k = 696.678 K and $\delta\epsilon^* = 0$; (b) ϵ^*_{12}/k = 678 K, $\delta\epsilon^*/k$ = 198.3 K, and $q = 10$; (c) ϵ^*_{12}/k = 666 K, $\delta\epsilon^*/k$ = 318.72 K, and $q = 10$; (d) ϵ^*_{12}/k = 657 K, $\delta\epsilon^*/k$ = 265.584 K, and $q = 6$. See text for discussion.

The second important point is that the calculated spinodal is too narrow. As can be seen in Figure 3b,c, adding "specific interaction character" to the model broadens the spinodal region but does not affect ϕ_c. In Figure 3b,c the calculated curves were determined in both cases with q = 10; in Figure 3b, $\delta\epsilon^*/k$ = 198.3 K and ϵ^*_{12}/k = 678 K, and in Figure 3c, $\delta\epsilon^*/k$ = 318.7 K and ϵ^*_{12}/k = 666 K. Once the entropy parameter q is fixed, $\delta\epsilon^*$ and ϵ^*_{12} act as a coupled pair; they must be chosen so that $\Delta\epsilon^*_T$ is negative at the LCST, where $\Delta\epsilon^*_T$ is defined as

$$\Delta\epsilon^*_T \equiv \epsilon^*_{11} + \epsilon^*_{22} - 2f^*_{12} = -\frac{1}{2}\frac{d^2\epsilon^*_T}{d\phi^2} \qquad (26)$$

Note that $\Delta\epsilon^*_T \rightarrow \Delta\epsilon^*$ as $T \rightarrow 0$. Decreasing ϵ^*_{12} and increasing $\delta\epsilon^*$ act to increase the amount of "specific interaction character" in the model. As can be seen, an excellent fit to the spinodal data has been obtained. In Figure 3d an equally good fit to the spinodal data is obtained with $q = 6$, $\delta\epsilon^*/k$ = 265.6 K, and ϵ^*_{12}/k = 657 K. As will be seen, the exact value of q is not important in establishing the ability of the model to correlate data. The parameters of Figure 3c,d are two sets of "best-fit" parameters.

In Figure 4 experimental spinodal data[17] for a different PVME/PS system are shown. Here both molecular weights are much higher than for data set 1: PS = 5.93 $\times 10^5$ and PVME = 1.1 $\times 10^6$ (data set 2). Since the molecular weights increased, the values of r_1 and r_2 increased proportionally (see eq 25 and Table I). Notice that the spinodal line has been pushed down to lower temperatures and the critical composition has been shifted to higher PVME concentration. In Figure 4a the calculated curve was determined by using the same energy parameters that were used in Figure 3a (no specific interaction, $\delta\epsilon^*$ = 0). Although the fit is reasonably good, a much better fit is obtained by using the same energy and entropy parameters as those in Figure 3c or 3d. This is a very stringent test of the theory because there are no adjustable parameters in this prediction.

Interaction Parameters

It is not generally recognized that a proper thermodynamic description of a binary polymer mixture requires four different χ interaction parameters; usually, only one of these is determined by a particular experimental measurement. The χ parameter that is measured depends on whether the experiment probes the free energy directly, its first derivative, or its second derivative. One parameter is associated with the free energy, two are associated with the two chemical potentials which depend on the first concentration derivative of the free energy; and one is associated with the spinodal which depends on the second derivative of the free energy. However, when one of the four parameters is known, the other three can be determined by rigorous thermodynamic relationships.[19]

In a small-angle neutron-scattering experiment, it is the latter χ associated with the spinodal that is determined

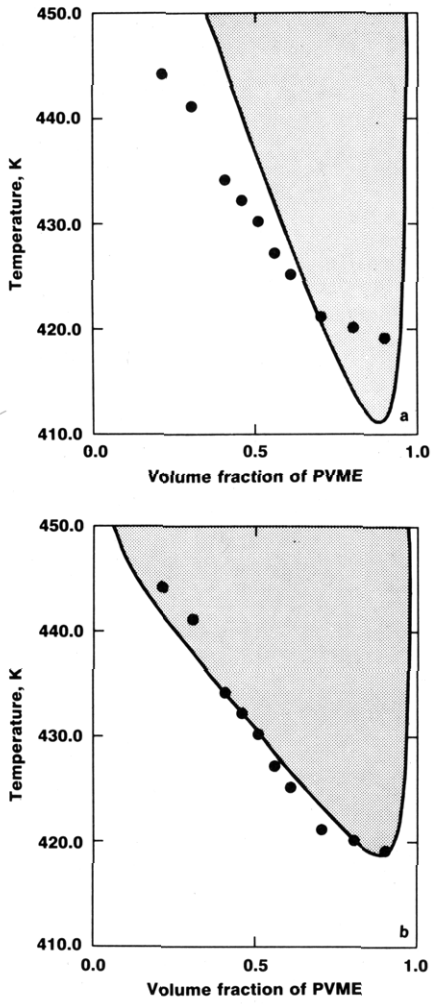

Figure 4. Comparison of experimental spinodal data[17] (solid circles, data set 2) and calculated spinodals for the PVME/PS system. Pure component parameters used in the calculations were all identical and are listed in Table I. Interaction parameters for Figure 4a were the same as for Figure 3a and those for Figure 4b were the same as for Figure 3c or 3d, i.e., no adjustable parameters. See text for discussion.

and it will be designated as χ_{sc} (the scattering χ). For the present model, χ_{sc} is given by

$$\chi_{sc} \equiv -\frac{1}{2}\frac{d^2(\beta f + s_{comb}/k)}{d\phi^2} = \tilde{\rho}\beta\Delta\epsilon^*_T + \frac{1}{2}f_{\phi\tilde{\rho}}{}^2 f_{\tilde{\rho}\tilde{\rho}}{}^{-1} \qquad (27)$$

where

$$\beta f_{\tilde{\rho}\tilde{\rho}} = \tilde{\rho}^{-1}[1/(1-\tilde{\rho}) + 1/r\tilde{\rho} - 2\beta\epsilon^*_T] \qquad (28a)$$

$$\beta f_{\tilde{\rho}\phi_1} = \beta(\epsilon^*_{22} - \epsilon^*_{11}) + (\phi_2 - \phi_1)\beta\Delta\epsilon^*_T + \frac{1}{\tilde{\rho}}\left(\frac{1}{r_1} - \frac{1}{r_2}\right) \qquad (29)$$

Notice that χ_{sc} approaches $\beta\Delta\epsilon^*$, the classical value of χ, at low temperatures.

With the equation of state, eq 17, it is easy to show that

$$\beta f_{\tilde{\rho}\tilde{\rho}} = -\frac{1}{r\tilde{\rho}^2} + \frac{1}{3} + \frac{1}{2}\tilde{\rho} + \frac{3}{5}\tilde{\rho}^2 + \ldots \qquad (28b)$$

As $r \to \infty$ it is obvious that $f_{\tilde{\rho}\tilde{\rho}}$ is positive for all allowable values of $\tilde{\rho}$. For finite r, eq 28 must be check numerically for positiveness because $f_{\tilde{\rho}\tilde{\rho}}$ will eventually become negative at low densities (produces a maximum rather than a mimimum in the free energy). At finite pressures, a stable state always exists (either gas or liquid below the gas–liquid critical point), but in our zero-pressure formulation of the present theory, the high-density phase (liquid) will eventually become thermodynamically unstable at high enough temperatures. Introducing pressure is easily accommodated by beginning with the Gibbs rather than the Helmholtz free energy in eq 1.

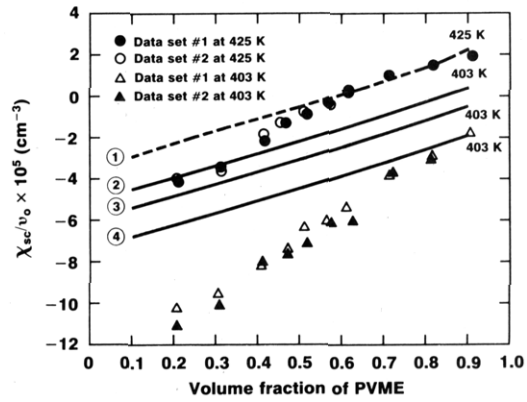

Figure 5. Comparison of experimental (symbols) and calculated (lines) χ interaction parameters as a function of composition and temperature for the PVME/PS system. All four sets of parameters used in Figure 3 were selected so that the LCST of 425 K was correctly predicted. All calculated (dimensionless) χ interaction parameters were divided by 18.4 cm^3/mol. The calculated curve (1) at 425 K, the dashed curve, is the same for all four sets of parameters. At 403 K, curve (2) corresponds to the parameters in Figure 3a, curve (3) corresponds to the parameters in Figure 3b, curve (4) corresponds to the parameters in Figure 3c or 3d. See text for discussion.

In the previous section it was stated that the critical composition ϕ_c for a LCST should be rich in the component with the smaller ϵ^*_{ii}, or equivalently, the smaller characteristic temperature T^*_i. The explanation is revealed in the two terms that comprise χ_{sc}. At a given temperature $\Delta\epsilon^*_T$ in the first term is a constant independent of composition, but $\tilde{\rho}$ varies with composition through its dependence on the compositionally dependent ϵ^*_T (see eq 17 and 18); $\tilde{\rho}$ and ϵ^*_T will usually attain their maximum and minimum values at the compositional end points ($\phi_1 = 0$ and 1). If the energetics are favorable ($\Delta\epsilon^*_T < 0$) and a LCST is obtained, $\tilde{\rho}\Delta\epsilon^*_T$ becomes less negative (less favorable) at compositions rich in the component with the smaller ϵ^*_{ii} since $\tilde{\rho}_i < \tilde{\rho}_j$ when $\epsilon^*_{ii} < \epsilon^*_{jj}$. Thus, the critical composition is shifted in that direction. (If $\epsilon^*_{ii} = \epsilon^*_{jj}$, then $\tilde{\rho}_i < \tilde{\rho}_j$ when $r_i < r_j$, but the value of r has little effect on $\tilde{\rho}$ for $r > 100$.) In the second term, the factor $f_{\tilde{\rho}\tilde{\rho}}{}^{-1}$ is positive and proportional to the isothermal compressibility (see eq 22); it also increases as $\tilde{\rho}$ decreases, tending to make χ_{sc} more positive and less favorable at compositions rich in the smaller ϵ^*_{ii} component. Arbitrarily selecting component 1 so that $\epsilon^*_{11} < \epsilon^*_{22}$, we see that $f_{\tilde{\rho}\phi_1}$ also increases in magnitude as $\phi_1 \to 1$ for a LCST type situation ($\Delta\epsilon^*_T < 0$). All of the equation of state contributions to χ_{sc} conspire to make it more positive (less favorable) on the composition side with the lower ϵ^*_{ii} and $\tilde{\rho}_i$. In summary, it is the asymmetry in the pure component parameters ϵ^*_{11} and ϵ^*_{22} that largely control the position of the critical composition of a LCST system. The two major consequences of these equation of state effects are that ϕ_c will be rich in the component with the smaller ϵ^*_{ii} or T^*_i and χ_{sc} is composition dependent.

Introducing specific interactions to the LF model has no effect on the critical composition. Specific interactions only affect the magnitude and temperature dependence of $\Delta\epsilon^*_T$, which is independent of composition.

The interaction parameter χ_{sc} has been experimentally determined at a variety of temperatures and compositions for data sets 1 and 2.[17] Little or no dependence of χ_{sc} on

molecular weight was observed. In Figure 5, χ_{sc} data are plotted as a function of composition for data sets 1 and 2 at 425 K, the LCST for data set 1, and at 403 K. Also shown are the calculated values of χ_{sc} for the parameter sets in Figures 3 used to fit the spinodal data (set 1). Since the experimental χ_{sc} data are in units of reciprocal volume, the calculated (dimensionless) χ_{sc} values were scaled by an appropriate scale factor so as to secure agreement between experimental and theoretical values at the critical composition ($\phi_{PVME} = 0.8$). Note that the calculated χ_{sc} values at 425 K all fall on the same line (curve 1). The significance of this result is that the compositional dependence of χ_{sc} is independent of the specific interaction and is controlled by equation of state effects. Since all of interaction parameters (ϵ^*_{12}, $\delta\epsilon^*$, and q) were selected so that the LCST of 425 K was correctly predicted, all four parameter sets yield the same calculated values of χ_{sc} at all other compositions. Notice, however, that the calculated values of χ_{sc} at 403 K are quite different (curves 2, 3, and 4). Curve 2 corresponds to the parameters used in Figure 3a, curve 3 corresponds to the parameters used in Figure 3b, and curve 4 corresponds to the parameters used in Figure 3c and 3d. The temperature dependence of χ_{sc} depends on the amount of specific interaction character that is introduced. Curve 4 illustrates that there are many combinations of the parameters q, ϵ^*_{12} and $\delta\epsilon^*$ that will give acceptable fits to the spinodal data and yield essentially the same temperature dependence for χ_{sc}. As the temperature increases beyond 425 K, better agreement between calculated and experimental χ_{sc} values is obtained for the "best-fit" parameters of Figure 3c and 3d. This is why the spinodal data on the PS-rich (and high temperature) part of the spinodal line is fit so well in Figures 3c, 3d, and 4b.

For completeness, the chemical potentials and their associated χ interaction parameters are given:

$$\mu_1 = r_1[f + \phi_2(\mathrm{d}f/\mathrm{d}\phi_1)]$$

$$\beta\mu_1 = \ln \phi_1 + (1 - r_1/r_2)\phi_2 + r_1\tilde{\rho}\beta\Delta\epsilon^*_T\phi_2^2 + r_1[-\tilde{\rho}\beta\epsilon^*_{11} + (1 - \tilde{\rho}) \ln (1 - \tilde{\rho})/\tilde{\rho} + \ln \tilde{\rho}/r_1] \quad (30)$$

The other chemical potential, μ_2, is obtained from eq 30 by interchange of the indexes 1 and 2.

In an experiment that probes the chemical potential, such as osmotic pressure, the two χ parameters that can be determined are $\chi_{\mu 1}$ and $\chi_{\mu 2}$ and are defined as[20]

$$\beta\Delta\mu_1 = \ln \phi_1 + (1 - r_1/r_2)\phi_2 + r_1\chi_{\mu 1}\phi_2^2$$

$$\beta\Delta\mu_2 = \ln \phi_2 + (1 - r_2/r_1)\phi_1 + r_2\chi_{\mu 2}\phi_1^2 \quad (31)$$

Since the reference chemical potential is usually taken to be the pure fluid, we have

$$\Delta\mu_i \equiv \mu_i - \mu_i^\circ \equiv \mu_i - \mu_i(\phi_i{=}1) \quad (32)$$

which for the generalized LF model becomes

$$\beta\Delta\mu_1 = \ln \phi_1 + (1 - r_1/r_2)\phi_2 + r_1\tilde{\rho}\beta\Delta\epsilon^*_T\phi_2^2 + r_1[-\tilde{\rho}\beta\epsilon^*_{11} + (1 - \tilde{\rho}) \ln (1 - \tilde{\rho})/\tilde{\rho} + \ln \tilde{\rho}/r_1 + \tilde{\rho}_1\beta\epsilon^*_{11} - (1 - \tilde{\rho}_1) \ln (1 - \tilde{\rho}_1)/\tilde{\rho}_1 - \ln \tilde{\rho}_1/r_1] \quad (33)$$

where $\tilde{\rho}_1$ is the reduced density of the pure component 1. Comparing eq 31 and 33, we see that

$$\chi_{\mu 1} = \tilde{\rho}\beta\Delta\epsilon^*_T + [\beta\epsilon^*_{11}(\tilde{\rho}_1 - \tilde{\rho}) + (1 - \tilde{\rho}) \ln (1 - \tilde{\rho})/\tilde{\rho} - (1 - \tilde{\rho}_1) \ln (1 - \tilde{\rho}_1)/\tilde{\rho}_1 + \ln (\tilde{\rho}/\tilde{\rho}_1)/r_1]/\phi_2^2 \quad (34)$$

and $\chi_{\mu 2}$ is obtained by interchanging the indexes 1 and 2 above. It can be shown by thermodynamic arguments[19] that

$$\chi_{sc}(\phi_i{=}1) = \chi_{\mu i}(\phi_i{=}1) \quad (35)$$

The classical or Flory–Huggins free energy of mixing Δf_{FH} defines the fourth interaction parameter χ:

$$\beta\Delta f_{FH} = -s_{comb}/k + \phi_1\phi_2\chi \quad (36)$$

where χ is linearly related to the chemical potential parameters by[19]

$$\chi = \phi_2\chi_{\mu 1} + \phi_1\chi_{\mu 2} \quad (37)$$

In the classical and ten Brinke–Karasz models, χ is independent of composition and

$$\chi = \chi_{\mu 1} = \chi_{\mu 2} = \chi_{sc} \quad (38)$$

Equation 38 is approached as a limit at low temperatures for the LF model ($\chi \to \beta\Delta\epsilon^*$).

Heat Capacities

The heat of mixing (Δh) per mer for the generalized LF model is

$$\Delta h = -\tilde{\rho}\epsilon^*_\theta + \tilde{\rho}_1\phi_1\epsilon^*_{11} + \tilde{\rho}_2\phi_2\epsilon^*_{22} \quad (39)$$

where

$$\epsilon^*_\theta \equiv \phi_1^2\epsilon^*_{11} + 2\phi_1\phi_2(\epsilon^*_{12} + \theta\delta\epsilon^*) + \phi_2^2\epsilon^*_{22} \quad (40)$$

The definition of ϵ^*_θ should be compared with the definitions of ϵ^* and ϵ^*_T given in eq 4 and 18. The excess heat capacity (Δc_p) is given by

$$\Delta c_p = \mathrm{d}\Delta h/\mathrm{d}T \quad (41)$$

which yields

$$\Delta c_p = z\phi_1\phi_2\tilde{\rho}(\beta\delta\epsilon)^2\theta(1 - \theta)k + \epsilon^*_\theta\tilde{\rho}\alpha - \phi_1\epsilon^*_{11}\tilde{\rho}_1\alpha_1 - \phi_2\epsilon^*_{22}\tilde{\rho}_2\alpha_2 \quad (42a)$$

where α_i is the thermal expansion coefficient of component i. With the relationship

$$T\alpha\tilde{\rho} = \beta\epsilon^*_T/f_{\tilde{p}\tilde{p}} \quad (43)$$

eq 42a can be rewritten as

$$\Delta c_p/k = z\phi_1\phi_2\tilde{\rho}(\beta\delta\epsilon)^2\theta(1 - \theta) + (\beta\epsilon^*_\theta)(\beta\epsilon^*_T)/f_{\tilde{p}\tilde{p}} - \phi_1(\beta\epsilon^*_{11})^2/f_{\tilde{p}\tilde{p}}(\phi_1{=}1) - \phi_2(\beta\epsilon^*_{22})^2/f_{\tilde{p}\tilde{p}}(\phi_2{=}1) \quad (42b)$$

Equations 22 and 42b illustrate how the finite compressibility of the mixture and of the pure components contributes to Δc_p. Negative contributions to Δc_p can come from only the pure-component terms (last two terms) since the first two terms are intrinsically positive.

Δc_p was calculated for the PVME/PS system for the four sets of parameters given in Figure 3. For the parameters of Figure 3a (no specific interactions), $\Delta c_p < 0$, but $\Delta c_p > 0$ for the other three parameter sets with specific interactions. Unfortunately, all calculated Δc_p values are very small. For the "best fit" parameters of Figure 3c,d, the calculated values of Δc_p were nearly identical and of the order of 10^{-4} cal/g, a value that is probably not experimentally detectable. Although Δc_p measurements have not been carried out on the PVME/PS system, two other miscible polymer blend systems have been investigated by Barnum et al.,[21] and in both systems they found that $\Delta c_p > 0$ with Δc_p of the order of 10^{-2} cal/g.

Summary

In the original LF model the interaction between dissimilar components, the 1–2 interaction, was a purely energetic one. In the generalization presented here, the 1–2 interaction has an entropic component that is temperature dependent. This generalization does not significantly

affect the compositional dependence of the χ interaction parameters but does affect their temperature dependence. There are four different χ parameters associated with a binary mixture, and all have been determined here for the generalized LF model.

The new model has been critically compared with recent small-angle neutron-scattering data on the polymer blend system poly(vinyl methyl ether)/polystyrene (PVME/PS).[17] The conclusions of this comparison are as follows:

Spinodal phase diagrams for this LCST system can be quantitatively calculated (Figure 3). Phase diagrams for other molecular weight combinations can now be predicted with confidence (no adjustable parameters) as demonstrated in Figure 4b.

The critical composition ϕ_c is a function of only the pure-component properties; without any adjustable parameters, the LF model correctly predicts ϕ_c. The ϕ_c is largely determined by the asymmetry in the characteristic temperatures (T^*_i) of the pure components. The model predicts that ϕ_c is rich in the component with the smaller T^*_i (PVME) as observed, whereas classical (incompressible) theories predict that ϕ_c is determined by size parameters and should be rich in the lower molecular weight component (PS).

The compositional and temperature dependence of the χ interaction parameters is accurately predicted for PVME-rich compositions, but deviations occur for PS-rich compositions (see Figure 5). The compositional dependence of the χ interaction parameters is controlled by equation of state effects and not specific interactions.

Calculated excess heat capacities are small ($\sim 10^{-4}$ cal/g) and positive.

We have demonstrated that the new LF model for a binary mixture is essentially a two-parameter theory. Both are energetic parameters. One parameter, ϵ_{12}, measures the strength of the nonspecific 1–2 interaction whereas $\epsilon_{12} + \delta\epsilon$ measures the strength of the specific 1–2 interaction. A third parameter that is entropic in nature (q), once chosen, defines the values of ϵ_{12} and $\delta\epsilon$ that are required to fit the data. The goodness of fit that can be achieved appears to be independent of q as long as $q \geq 1$ (see Figures 3, 4, and 5). When $\delta\epsilon = 0$, there is no entropic contribution to the 1–2 interaction, and the model reduces to the original LF model.

Although specific interactions have been added to the LF model and play a important role in determining the temperature dependence of the interaction parameters, unfavorable compressibility (equation of state) effects are still the primary reason this system exhibits a LCST.

On the basis of our experience with the PVME/PS system, the inclusion of specific interactions and the associated entropy effects has significantly improved the LF model. This has been achieved while maintaining the model's simplicity.

Although the treatment here is of the mean-field type, there is a local ordering and a nonrandom aspect to the model. For example, the probability that a mer belonging to component 1 will form a specific interaction with a mer in an adjacent site belonging to component 2 equals $\theta\tilde{p}\phi_2$; ϕ_2 is the fraction of type 2 mers, $\tilde{p}$ is the fraction of all sites occupied, and only a fraction θ of the 1–2 interactions are specific. Both order parameters, $\tilde{p}$ and θ, are functions of temperature, and both approach unity as the temperature is lowered; thus, the solution becomes more ordered (more specific interactions) at low temperatures. Also $\tilde{p}$ depends on composition, so that at a fixed temperature the degree of order varies with composition.

Is our generalization of the LF model for specific interactions realistic? The ratio of the number of nonspecific 1–2 interactions to specific interactions is given by

$$\frac{\text{no. of nonspecific interactions}}{\text{no. of specific interactions}} = \frac{1-\theta}{\theta} = q\exp(-\beta\delta\epsilon) \tag{44}$$

This result is consistent with the Boltzmann distribution law of statistical mechanics; $\delta\epsilon$ is the energy difference between the two states, and q is the ratio of the statistical degeneracies of the two states. Quasi-chemical equations[15] are also of the same form but with $q = 2$.

What we have ignored is the possibility of specific interactions in the pure components. Certainly this is a possible future generalization, but the present theory appears to work remarkably well without invoking specific interactions among the pure components. Recently, Painter et al.[22] have criticized mixture theories of strongly interacting components that ignore this possibility of specific interactions among the pure components. In our view it is a much more serious approximation to ignore equation of state effects. All real mixtures are compressible, and if one or more of the components are polymers, equation of state effects play a very important role (if not dominate) in determining the phase behavior of these systems.

Acknowledgment. We acknowledge the helpful assistance of Robert Miller in carrying out many of the numerical calculations.

Registry No. PS, 9003-53-6; PVME, 9003-09-2.

References and Notes

(1) Rowlinson, J. S.; Swinton, F. L. *Liquids and Liquid Mixtures*; Butterworths: London, 1982; p 117.
(2) Sanchez, I. C. *Polymer Compatibility and Incompatibility: Principles and Practices*; MMI Press Symposium Series 2; Solc, K., Ed.; Harwood: New York, 1982; p 59.
(3) Sanchez, I. C. *Encyclopedia of Physical Science and Technology*; Academic Press: New York, 1987; Vol. XI, p 1.
(4) Flory, P. J.; Orwoll, R. A.; Vrij, A. *J. Am. Chem. Soc.* **1964**, *86*, 3515.
(5) Flory, P. J. *J. Am. Chem. Soc.* **1965**, *87*, 1833.
(6) Eichinger, B. E.; Flory, P. J. *Trans. Faraday Soc.* **1968**, *64*, 2035.
(7) Flory, P. J. *Discuss. Faraday Soc.* **1970**, *49*, 7.
(8) Sanchez, I. C.; Lacombe, R. H. *J. Phys. Chem.* **1976**, *80*, 2352, 2568.
(9) Sanchez, I. C.; Lacombe, R. H. *J. Polym. Sci., Polym. Lett. Ed.* **1977**, *15*, 71.
(10) Sanchez, I. C.; Lacombe, R. H. *Macromolecules* **1978**, *11*, 1145.
(11) The interactions do not have to be "strong" to have energetically induced ordering in a solution. As quasi-chemical calculations show, any asymmetry in the attractive interaction energies between components ($\epsilon_{11} \neq \epsilon_{22} \neq \epsilon_{12}$) is sufficient to induce some local ordering.
(12) Panayiotou, C.; Vera, J. H. *Fluid Phase Equilib.* **1980**, *5*, 55.
(13) Renuncio, J. A. R.; Prausnitz, J. M. *Macromolecules* **1976**, *9*, 895.
(14) Panayiotou, C. G. *Macromolecules* **1987**, *20*, 861.
(15) Guggenheim, E. A. *Proc. R. Soc. London, A* **1944**, *A183*, 213.
(16) ten Brinke, G.; Karasz, F. E. *Macromolecules* **1984**, *17*, 815.
(17) Han, C. C.; Baurer, B. J.; Clark, J. C.; Muroga, Y.; Matsushita, Y.; Okada, M.; Tran-Cong, Q.; Chang, T.; Sanchez, I. C. *Polymer* **1988**, *29*, 2002.
(18) Uriarte, C.; Eguiazabal, J. I.; Llanos, M.; Iribarren, J. I.; Iruin, J. J. *Macromolecules* **1987**, *20*, 3038.
(19) Sanchez, I. C. *Polymer*, in press.
(20) In practice, r_1 and r_2 are replaced by the respective molar volumes of the components, and $kT\chi_\mu$ has units of energy density.
(21) Barnum, R. S.; Goh, S. H.; Barlow, J. W.; Paul, D. R. *J. Polym. Sci., Polym. Lett. Ed.* **1985**, *23*, 395.
(22) Painter, P. C.; Park, Y.; Coleman, M. M. *Macromolecules* **1988**, *21*, 66.